This journal is (c) The Royal Society of Chemistry and The Centre National de la Recherche Scientifique, 2010

Supporting information to be published electronically

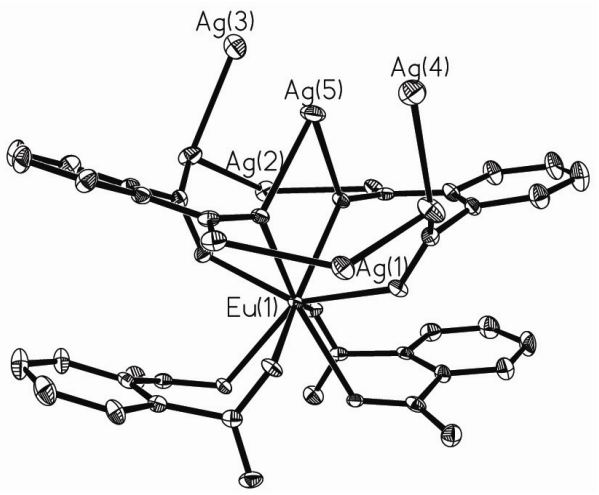

Fig. S1 The asymmetric unit of complex **1**. Thermal ellipsolid is of 30% probability.

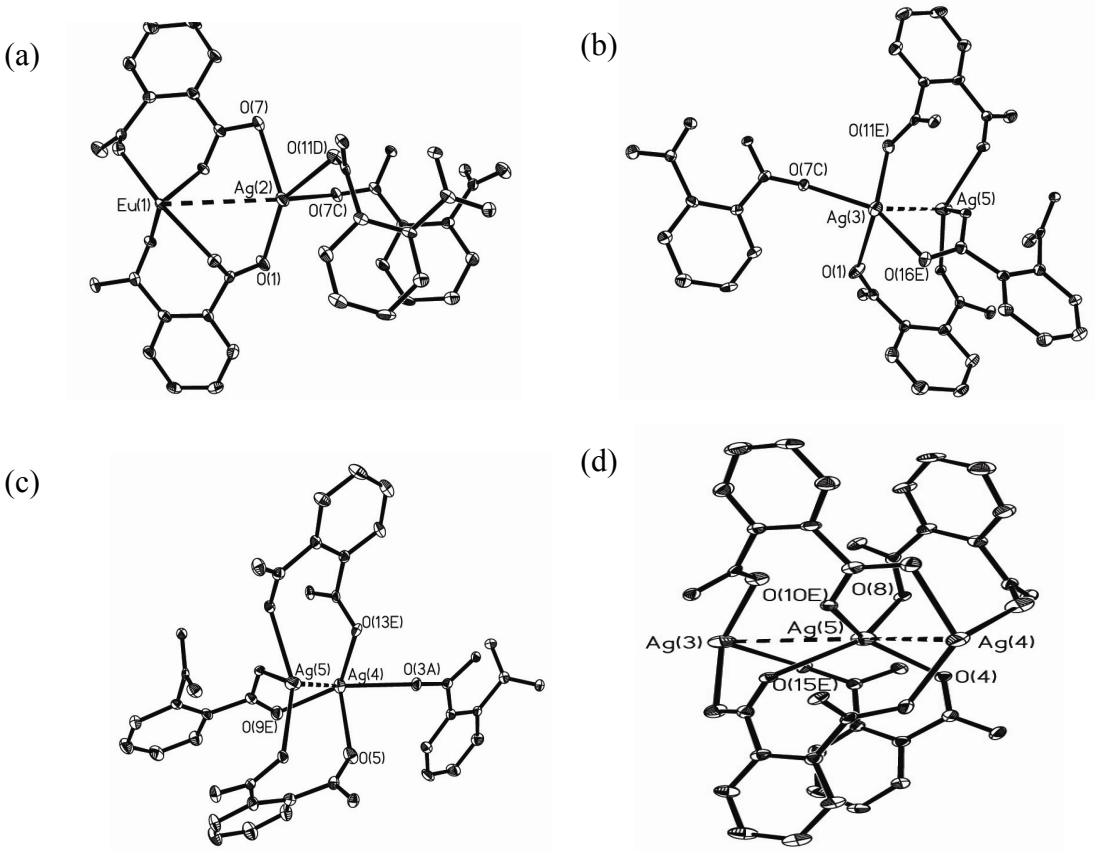

Fig. S2 The local coordination enviroment around Ag(I) ions in complex **1**. Thermal ellipsolid is of 30% probability.

If taking into the M…M interaction, the Ag(I) ion may be considered to be 5-coordinated or 6-coordinated. Thus, the coordination modes of five Ag(I) ions in complex **1** can be divided into three types:(a) the first one involves two Ag(I) ions (Ag(1) and Ag(2) ions) with four Ag-O bonds and one Eu…Ag interacion (Fig.1b in the text and Fig. S2a); (b) the second one includes Ag (3) and Ag (4) ions with four Ag-O bonds and one Ag…Ag interacion (Fig. S2b and Fig. S2c); (c) the last one involves Ag (5) ion, which is 6-coordinated with four Ag-O bonds and two

Ag…Ag interacion(Fig. S2d).

Table S1. The selected bond lengths (Å) around Ln(III) and Ag(I) ions in complexes **1–4**

Complex	Ln-O		Ag-O			
1	Eu(1)-O(12)	2.337(4)	Ag(1)-O(5)	2.302(4)	Ag(2)-O(1)	2.298(4)
	Eu(1)-O(6)	2.331(4)	Ag(1)-O(13)[a]	2.335(4)	Ag(2)-O(11)[c]	2.317(4)
	Eu(1)-O(14)	2.338(4)	Ag(1)-O(3)	2.456(4)	Ag(2)-O(7)	2.472(4)
	Eu(1)-O(2)	2.334(4)	Ag(1)-O(3)[b]	2.544(4)	Ag(2)-O(7)[d]	2.568(4)
	Eu(1)-O(15)	2.428(4)	Ag(3)-O(16)[e]	2.345(4)	Ag(4)-O(9)[e]	2.383(4)
	Eu(1)-O(10)	2.438(3)	Ag(3)-O(11)[e]	2.397(4)	Ag(4)-O(13)[e]	2.397(4)
	Eu(1)-O(8)	2.440(4)	Ag(3)-O(7)[d]	2.430(4)	Ag(4)-O(3)[b]	2.481(4)
	Eu(1)-O(4)	2.455(4)	Ag(3)-O(1)	2.564(4)	Ag(4)-O(5)	2.486(4)
			Ag(5)-O(15)[e]	2.397(4)	Ag(5)-O(4)	2.421(4)
			Ag(5)-O(8)	2.403(3)	Ag(5)-O(10)[e]	2.431(4)
2	Yb(1)-O(12)	2.255(13)	Ag(1)-O(5)	2.322(15)	Ag(2)-O(1)	2.313(14)
	Yb(1)-O(6)	2.238(14)	Ag(1)-O(13)[a]	2.337(12)	Ag(2)-O(11)[c]	2.309(13)
	Yb(1)-O(14)	2.256(12)	Ag(1)-O(3)	2.442(14)	Ag(2)-O(7)	2.456(15)
	Yb(1)-O(2)	2.258(12)	Ag(1)-O(3)[b]	2.561(13)	Ag(2)-O(7)[d]	2.584(12)
	Yb(1)-O(15)	2.396(13)	Ag(3)-O(16)[e]	2.334(15)	Ag(4)-O(13)[e]	2.358(14)
	Yb(1)-O(10)	2.384(12)	Ag(3)-O(11)[e]	2.371(15)	Ag(4)-O(9)[e]	2.392(15)
	Yb(1)-O(8)	2.401(11)	Ag(3)-O(7)[d]	2.448(13)	Ag(4)-O(3)[b]	2.475(12)
	Yb(1)-O(4)	2.405(11)	Ag(3)-O(1)	2.553(14)	Ag(4)-O(5)	2.483(14)
			Ag(5)-O(15)[e]	2.392(12)	Ag(5)-O(4)	2.406(12)
			Ag(5)-O(8)	2.388(11)	Ag(5)-O(10)[e]	2.399(12)
3	Er(1)-O(12)	2.284(8)	Ag(1)-O(5)	2.314(9)	Ag(2)-O(1)	2.310(10)
	Er(1)-O(6)	2.283(8)	Ag(1)-O(13)[a]	2.332(9)	Ag(2)-O(11)[c]	2.311(8)
	Er(1)-O(14)	2.292(8)	Ag(1)-O(3)	2.445(9)	Ag(2)-O(7)	2.453(9)
	Er(1)-O(2)	2.292(8)	Ag(1)-O(3)[b]	2.555(9)	Ag(2)-O(7)[d]	2.572(9)
	Er(1)-O(15)	2.397(7)	Ag(3)-O(16)[e]	2.327(10)	Ag(4)-O(9)[e]	2.371(10)
	Er(1)-O(10)	2.415(8)	Ag(3)-O(11)[e]	2.397(9)	Ag(4)-O(13)[e]	2.376(9)
	Er(1)-O(8)	2.423(8)	Ag(3)-O(7)[d]	2.436(8)	Ag(4)-O(3)[b]	2.491(9)
	Er(1)-O(4)	2.424(8)	Ag(3)-O(1)	2.567(10)	Ag(4)-O(5)	2.495(10)
			Ag(5)-O(15)[e]	2.385(7)	Ag(5)-O(4)	2.418(8)
			Ag(5)-O(8)	2.397(8)	Ag(5)-O(10)[e]	2.408(7)
4	Ho(1)-O(12)	2.280(9)	Ag(1)-O(5)	2.305(10)	Ag(2)-O(1)	2.311(9)
	Ho(1)-O(6)	2.282(9)	Ag(1)-O(13)[a]	2.322(9)	Ag(2)-O(11)[c]	2.315(9)
	Ho(1)-O(14)	2.305(9)	Ag(1)-O(3)	2.453(10)	Ag(2)-O(7)	2.462(10)
	Ho(1)-O(2)	2.308(9)	Ag(1)-O(3)[b]	2.544(10)	Ag(2)-O(7)[d]	2.578(9)
	Ho(1)-O(15)	2.390(9)	Ag(3)-O(16)[e]	2.333(10)	Ag(4)-O(9)[e]	2.381(10)
	Ho(1)-O(10)	2.412(9)	Ag(3)-O(11)[e]	2.394(10)	Ag(4)-O(13)[e]	2.400(10)
	Ho(1)-O(8)	2.414(8)	Ag(3)-O(7)[d]	2.449(9)	Ag(4)-O(5)	2.502(10)
	Ho(1)-O(4)	2.424(8)	Ag(3)-O(1)	2.551(10)	Ag(4)-O(3)[b]	2.505(10)
			Ag(5)-O(15)[e]	2.408(9)	Ag(5)-O(4)	2.410(8)
			Ag(5)-O(8)	2.402(8)	Ag(5)-O(10)[e]	2.421(9)

Symmetry transformations used to generate equivalent atoms: [a] -x+1, -y, -z+1; [b] -x, -y, -z+1; [c] -x+1, -y+1, -z;

[d] -x, -y+1, -z; [e] x-1, y, z; [f] x+1, y, z.

Table S2 Structure data of four bdc^{2-} anions in each of complexes **1–4**

Coordination mode	μ_7–bdc								μ_5–bdc							
Complex	**1**		**2**		**3**		**4**		**1**		**2**		**3**		**4**	
Angle between two carboxyl planes/ °	54.5	56.6	50.9	52.1	52.7	54.0	55.3	55.0	95.0	87.1	93.2	88.3	90.9	93.8	89.1	92.7
Angle between carboxyl and benzene ring plane / °	14.9	12.2	15.7	12.6	15.1	11.7	14.5	12.4	17.9	12.7	17.9	14.7	12.6	17.6	14.0	17.6
	57.5	52.5	53.4	50.4	54.8	79.7	55.3	50.3	82.6	96.8	79.2	100.0	99.4	80.4	99.2	80.7

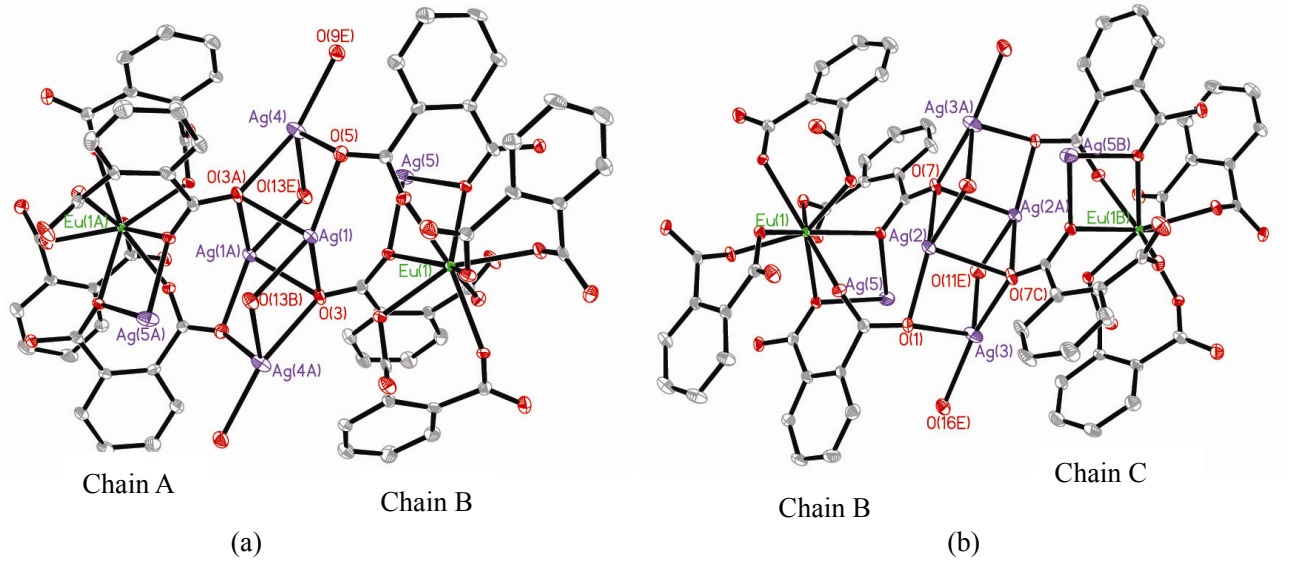

Fig. S3 The detail of interchain connection in complex **1**: (a) connection through Ag(1) and Ag(4) ions coordinating to the bdc^{2-} anions from intrachain; (b) connection through Ag(2) and Ag(3) ions coordinating to the bdc^{2-} anions from intrachain. Thermal ellipsolid is of 30% probability.

Firstly, the adjacent chain A and B are linked by Ag(1) and Ag(4) ions, and chain B is further linked through Ag(2) and Ag(3) ions with chain C, then chain C is linked with chain A, …… As a result, the repeated arrangement of chains …ABCABCABC… appears in the direction of $\vec{c}$, which results in formation of the 2D layer.

Table S3. The separations of M…M (Å) in complexes **1–4**

Complex	**1**		**2**		**3**		**4**	
Ln…Ag	Eu…Ag1	3.730(2)	Yb…Ag1	3.708(3)	Er…Ag1	3.724(2)	Ho…Ag1	3.724(1)
	Eu…Ag2	3.752(1)	Yb…Ag2	3.733(3)	Er…Ag2	3.746(2)	Ho…Ag2	3.749(2)
Ag…Ag	Ag3…Ag5	3.318(2)	Ag3…Ag5	3.297(3)	Ag3…Ag5	3.316(2)	Ag3…Ag5	3.312(3)
	Ag4…Ag5	3.324(2)	Ag4…Ag5	3.296(3)	Ag4…Ag5	3.319(2)	Ag4…Ag5	3.319(3)
	Ag1…Ag4	3.464(1)	Ag1…Ag4	3.432(2)	Ag1…Ag4	3.449(1)	Ag1…Ag4	3.448(2)
	Ag2…Ag3	3.426(1)	Ag2…Ag3	3.398(2)	Ag2…Ag3	3.410(2)	Ag2…Ag3	3.410(2)

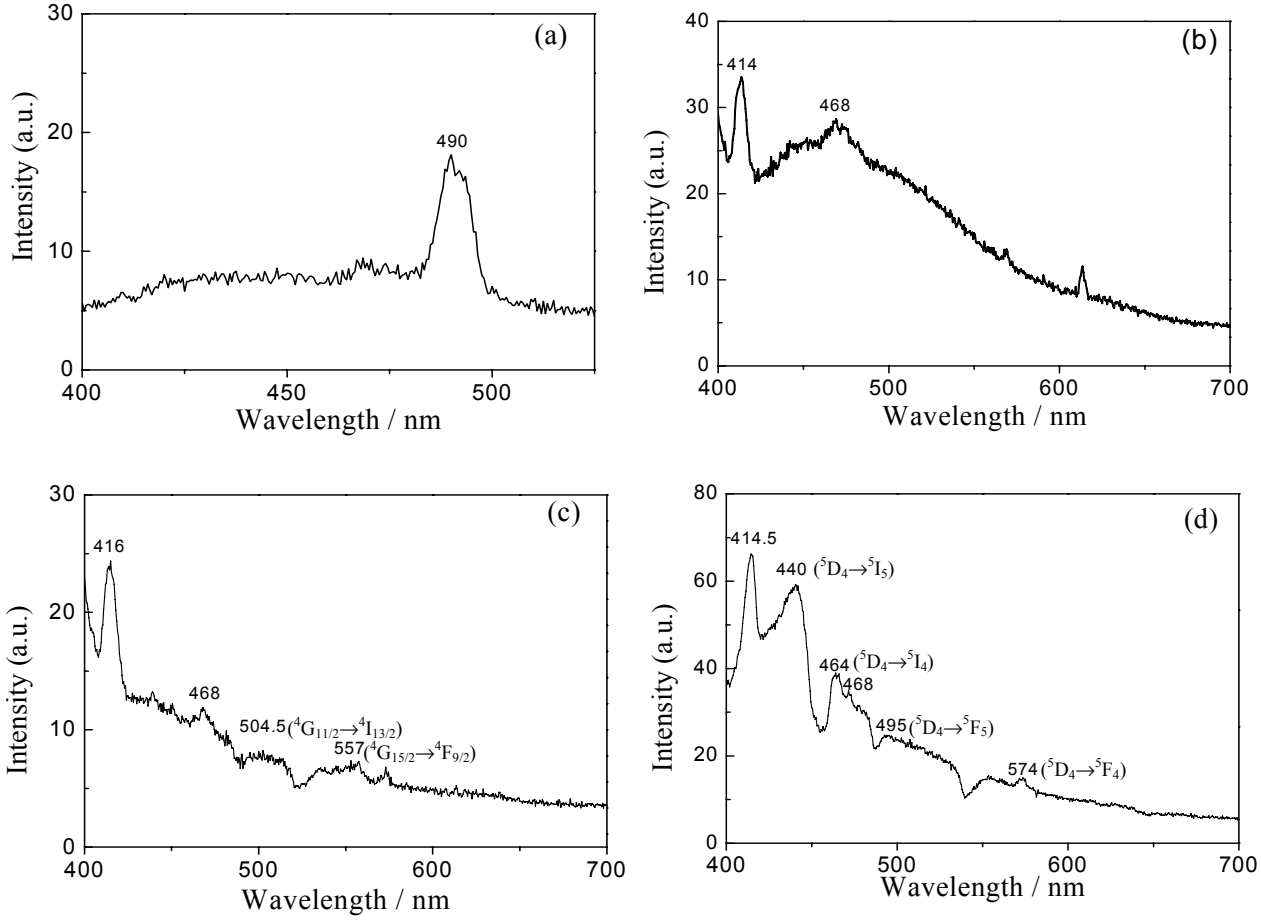

Fig. S4 The emission spectra of complex **1-4** in the visible region. (a) complex **1** (Eu-Ag), λ_{ex} = 298 nm; (b) complex **2** (Yb-Ag), λ_{ex} = 380 nm; (c) complex **3** (Er-Ag), λ_{ex} = 383 nm; (d) complex **4** (Ho-Ag), λ_{ex} = 381.5 nm.

With λ_{ex} = 298nm, the luminescence of ligand has been completely quenched and the emission of Ag-block shifts red (λ_{max} = 490 nm) in complex **1** (Fig. S4a), which suggests that the energy transfer from ligand and Ag-block to Eu(III) ion take place effectively, *i.e.*, sensizitation of liagnd and Ag-block to Eu(III)ion. With λ_{ex} = 380 nm, complex **2** exhibit two emission bands in the visible region (Fig. S4b). The one at 414 nm is assigned to the LLCT, and the other at 468 nm is attributed to LMCT of Ag-block because there is no emission peak at this position for the free ligand.[a] For complex **3** and **4**, except for the LLCT and LMCT transition, there present the *f-f* emission bands of corresponding Ln(III) ions in the visible region, but they are very weak (Fig. S4c and Fig. S4d). From the emission spectra of the complex **2-4**, we can find that emissions of ligand and Ag-block (Ag-ligand section) are observed, which suggests that the energy are mainly used as the luminescence of ligand and Ag-block and not effectively transferred to the Ln(III) ions.

[a] R. P. Feazell, C. E. Carson, and K. K. Klausmeyer, *Eur. J. Inorg. Chem*., 2005, 3287; F. T. Xie, H. Y. Bie, L. M. Duan, G. H. li, X. Zhang, J. Q. Xu, *Solid State Chem.*, 2005, **178**, 2858.

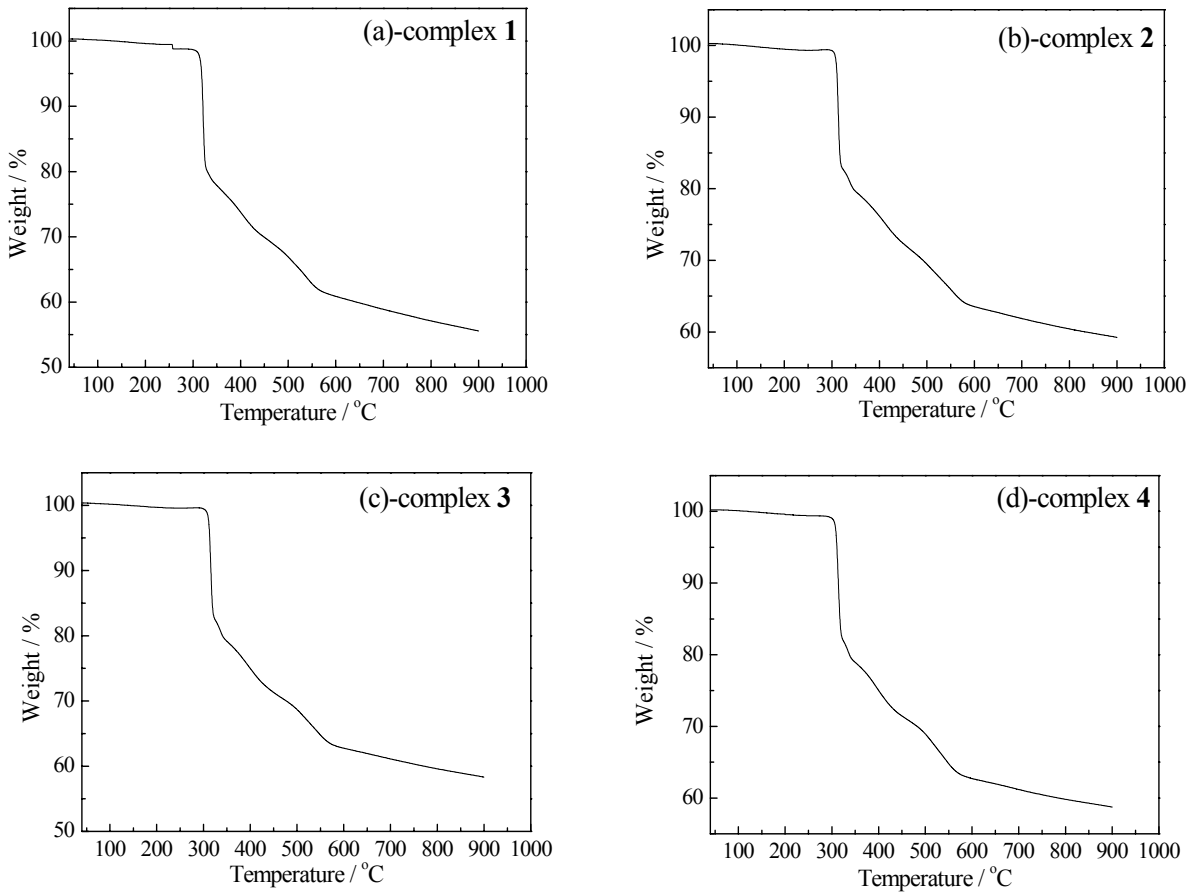

Fig. S5 The TG curves of complexes **1-4**.

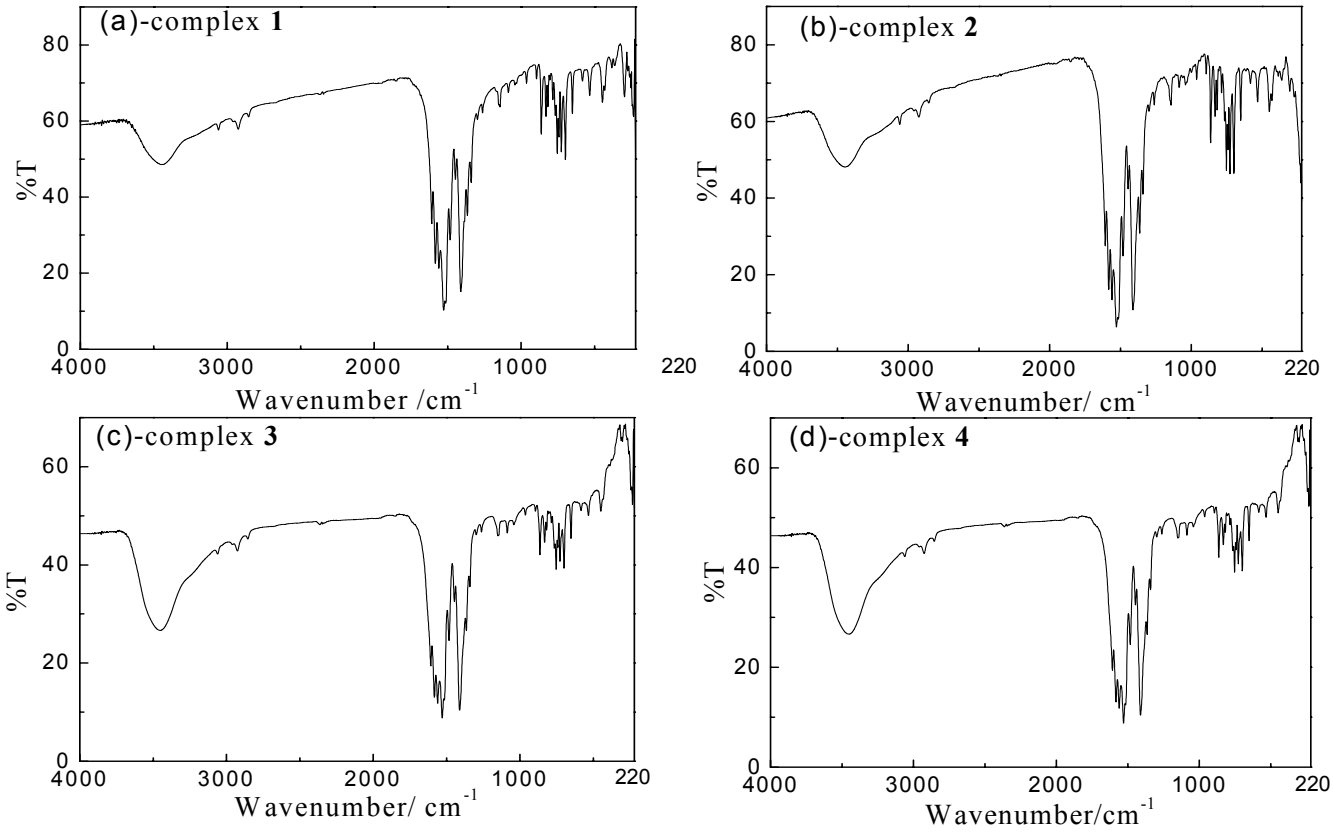

Fig. S6 The IR spectra of complexes **1-4**